

Fig. 1. Mirror positions and fields in a Fabry–Perot cavity.

the cavity length are due to the mirror displacements  $x_a(t)$  and  $x_b(t)$  which are measured with respect to reference planes  $a$  and  $b$ . The nominal light transit time and the free spectral range (FSR) of the cavity are defined by

$$T = \frac{L}{c}, \quad \omega_{\text{FSR}} = \frac{\pi}{T}. \quad (1)$$

The field incident upon the cavity and the field circulating in the cavity are described by plane waves with nominal frequency  $\omega$  and wavenumber  $k$  ( $k = \omega/c$ ). Variations in the laser frequency are denoted by  $\delta\omega(t)$ . We assume that the mirror displacements are much less than the nominal cavity length and that the deviations of the laser frequency are much less than the nominal frequency.

At any given place the electric field  $\mathcal{E}$  in the cavity oscillates at a very high frequency:  $\mathcal{E}(t) \propto e^{i\omega t}$ . For simplicity, we suppress the fast-oscillating factor and define the slowly-varying field as

$$E(t) = \mathcal{E}(t)e^{-i\omega t}. \quad (2)$$

To properly account for the phases of the propagating fields, their complex amplitudes must be defined at fixed locations, reference planes  $a_1$  and  $a_2$ , as shown in Fig. 1. (The small offset  $\epsilon$  is introduced for clarity and will be set to zero at the end of calculations.)

The equations for fields in the cavity can be obtained by tracing a wavefront during its complete round-trip in the cavity. The first propagation delay,  $\tau_1$ , corresponds to the light transit time from the reference plane  $a_2$  to the end mirror and back to  $a_2$ . The second propagation delay,  $\tau_2$ , corresponds to the light transit time from the reference plane  $a_2$  to the front mirror and back to  $a_2$ . They are given by

$$c\tau_1 = L - \epsilon + x_b(t - \tau_1), \quad (3)$$

$$c\tau_2 = \epsilon - x_a(t - \tau_2). \quad (4)$$

Then the fields in the cavity satisfy the equations:

$$E'(t) = -r_b E(t - 2\tau_1)e^{-2i\omega\tau_1}, \quad (5)$$

$$E(t) = -r_a E'(t - 2\tau_2)e^{-2i\omega\tau_2} + t_a E_{\text{in}}(t - 2\epsilon/c), \quad (6)$$

where  $r_a$  and  $r_b$  are the mirror reflectivities, and  $t_a$  is the transmissivity of the front mirror.

Because the field amplitudes  $E$  and  $E'$  do not change significantly over times of order  $x_{a,b}/c$ , the small variations in these amplitudes caused by the changes in propagation times due to mirror displacements can be neglected. Furthermore, the offset  $\epsilon$  can be set to zero, and Eqs. (5) and (6) can be combined yielding one equation for the cavity field

$$E(t) = t_a E_{\text{in}}(t) + r_a r_b e^{-2ik[L + \delta L(t)]} E(t - 2T). \quad (7)$$

Here  $\delta L(t)$  is the variation in the cavity length “seen” by the light circulating in the cavity,

$$\delta L(t) = x_b(t - T) - x_a(t). \quad (8)$$

Note that the time delay appears in the coordinate of the end mirror, but not the front mirror. This is simply a consequence of our placement of the laser source; the light that enters the cavity reflects from the end mirror first and then the front mirror.

There is still an arbitrariness in the position of the reference planes  $a$  and  $b$ . These reference plane can be chosen so that the nominal length of the Fabry–Perot cavity becomes an integer multiple of the laser wavelength, making  $e^{-2ikL} = 1$ . Then the equation for field dynamics in Fabry–Perot cavity becomes

$$E(t) = t_a E_{\text{in}}(t) + r_a r_b e^{-2ik\delta L(t)} E(t - 2T). \quad (9)$$

For  $\delta L = 0$ , Laplace transformation of both sides of Eq. (9) yields the basic cavity response function

$$H(s) \equiv \frac{\tilde{E}(s)}{\tilde{E}_{\text{in}}(s)} = \frac{t_a}{1 - r_a r_b e^{-2sT}}, \quad (10)$$

where tildes denote Laplace transforms.

### 3. Condition for resonance

The static solution of Eq. (9) is found by considering a cavity with fixed length ( $\delta L = \text{const}$ ) and an input laser field with fixed amplitude and frequency ( $A, \delta\omega = \text{const}$ ). In this case the input laser field and

the cavity field are given by

$$E_{\text{in}}(t) = Ae^{i\delta\omega t}, \quad (11)$$

$$E(t) = E_0e^{i\delta\omega t}, \quad (12)$$

where  $E_0$  is the amplitude of the cavity field,

$$E_0 = \frac{t_a A}{1 - r_a r_b \exp[-2i(T\delta\omega + k\delta L)]}. \quad (13)$$

The cavity field is maximized when the length and the laser frequency are adjusted so that

$$\frac{\delta\omega}{\omega} = -\frac{\delta L}{L}. \quad (14)$$

This is the well-known static resonance condition. The maximum amplitude of the cavity field is given by

$$\bar{E} = \frac{t_a A}{1 - r_a r_b}. \quad (15)$$

Light can also resonate in a Fabry–Perot cavity when its length and the laser frequency are changing. For a fixed amplitude and variable phase, the input laser field can be written as

$$E_{\text{in}}(t) = Ae^{i\phi(t)}, \quad (16)$$

where  $\phi(t)$  is the phase due to frequency variations,

$$\phi(t) = \int_0^t \delta\omega(t') dt'. \quad (17)$$

Then the steady-state solution of Eq. (9) is

$$E(t) = \bar{E}e^{i\phi(t)}, \quad (18)$$

where the amplitude  $\bar{E}$  is given by Eq. (15) and the phase satisfies the condition

$$\phi(t) - \phi(t - 2T) = -2k\delta L(t). \quad (19)$$

Thus resonance occurs when the phase of the input laser field is corrected to compensate for the changes in the cavity length due to the mirror motions. The associated laser frequency correction is equal to the Doppler shift caused by reflection from the moving mirrors

$$\delta\omega(t) - \delta\omega(t - 2T) = -2\frac{v(t)}{c}\omega, \quad (20)$$

where  $v(t)$  is the relative mirror velocity ( $v = d\delta L/dt$ ). The equivalent formula in the Laplace domain is

$$C(s)\frac{\delta\tilde{\omega}(s)}{\omega} = -\frac{\delta\tilde{L}(s)}{L}, \quad (21)$$

where  $C(s)$  is the normalized frequency-to-length transfer function which is given by

$$C(s) = \frac{1 - e^{-2sT}}{2sT}. \quad (22)$$

Eq. (21) is the condition for dynamic resonance. It must be satisfied in order for light to resonate in the cavity when the cavity length and the laser frequency are changing [15].

The transfer function  $C(s)$  has zeros at multiples of the cavity free spectral range,

$$z_n = i\omega_{\text{fsr}}n, \quad (23)$$

where  $n$  is integer, and therefore can be written as the infinite product,

$$C(s) = e^{-sT} \prod_{n=1}^{\infty} \left(1 - \frac{s^2}{z_n^2}\right), \quad (24)$$

which is useful for control system design.<sup>1</sup> The magnitude of this transfer function,

$$|C(s = i\Omega)| = \frac{\sin \Omega T}{\Omega T}, \quad (25)$$

for imaginary values of  $s$ -variable (Fourier domain) is shown in Fig. 2. Its phase is a linear function of frequency:  $\arg\{C(i\Omega)\} = -\Omega T$ .

To maintain resonance, changes in the cavity length must be compensated by changes in the laser frequency according to Eq. (21). If the frequency of such changes is much less than the cavity free spectral range,  $C(s) \approx 1$  and Eq. (21) reduces to the quasi-static approximation,

$$\frac{\delta\tilde{\omega}(s)}{\omega} \approx -\frac{\delta\tilde{L}(s)}{L}. \quad (26)$$

At frequencies above the cavity free spectral range,  $C(s) \propto 1/s$  and increasingly larger laser frequency changes are required to compensate for cavity length variations. Moreover, at multiples of the FSR  $C(s) = 0$  and no frequency-to-length compensation is possible.

<sup>1</sup> This formula is derived using the infinite-product representation for sine:  $\sin x = x \prod_{n=1}^{\infty} (1 - x^2/\pi^2 n^2)$ .

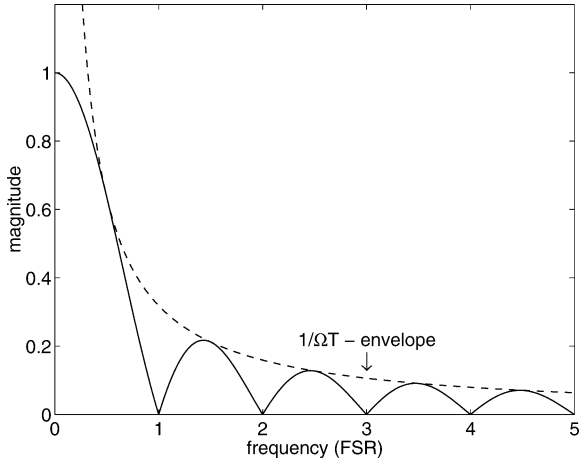


Fig. 2. Magnitude of  $C(s = i\Omega)$ . (The dashed line shows the decay of the maximum value of  $C(i\Omega)$  within each FSR, as a function of frequency.)

#### 4. Frequency response

In practice, Fabry–Perot cavities tend to deviate from resonance, and a negative-feedback control system is employed to reduce the deviations. For small deviations from resonance, the cavity field can be described as

$$E(t) = [\bar{E} + \delta E(t)]e^{i\phi(t)}, \quad (27)$$

where  $\bar{E}$  is the maximum field given by Eq. (15), and  $\delta E$  is a small perturbation ( $|\delta E| \ll |\bar{E}|$ ). Substituting this equation into Eq. (9), we see that the perturbation evolves in time according to

$$\begin{aligned} \delta E(t) - r_a r_b \delta E(t - 2T) \\ = -i r_a r_b \bar{E} [\phi(t) - \phi(t - 2T) + 2k\delta L(t)]. \end{aligned} \quad (28)$$

This equation is easily solved in the Laplace domain, yielding

$$\delta \tilde{E}(s) = -i r_a r_b \bar{E} \frac{(1 - e^{-2sT})\tilde{\phi}(s) + 2k\delta \tilde{L}(s)}{1 - r_a r_b e^{-2sT}}. \quad (29)$$

Deviations of the cavity field from its maximum value can be measured by the Pound–Drever–Hall (PDH) error signal which is widely utilized for feedback control of Fabry–Perot cavities [16]. The PDH signal is obtained by coherent detection of phase-modulated light reflected by the cavity. With the appropriate choice of the demodulation phase, the PDH

signal is proportional to the imaginary part of the cavity field,  $\delta E$ , and therefore can be written as

$$\delta \tilde{V}(s) \propto H(s) \left[ \frac{\delta \tilde{L}(s)}{L} + C(s) \frac{\delta \tilde{\omega}(s)}{\omega} \right], \quad (30)$$

where  $H(s)$  is given by Eq. (10). In the presence of length and frequency variations, feedback control will drive the error signal toward the null point,  $\delta \tilde{V} = 0$ , thus maintaining dynamic resonance according to Eq. (21).

The response of the PDH signal to either length or laser frequency deviations can be found from Eq. (30). The normalized length-to-signal transfer function is given by

$$H_L(s) = \frac{H(s)}{H(0)} = \frac{1 - r_a r_b}{1 - r_a r_b e^{-2sT}}. \quad (31)$$

A Bode plot (magnitude and phase) of  $H_L$  is shown in Fig. 3 for the LIGO [2] Fabry–Perot cavities with  $L = 4$  km,  $r_a = 0.985$ , and  $r_b = 1$ . The magnitude of the transfer function,

$$|H_L(i\Omega)| = \frac{1}{\sqrt{1 + F \sin^2 \Omega T}}, \quad (32)$$

is the square-root of the well-known Airy function with the coefficient of finesse  $F = 4r_a r_b / (1 - r_a r_b)^2$ . (In optics, the Airy function describes the intensity profile of a Fabry–Perot cavity [17].)

The transfer function  $H_L$  has an infinite number of poles:

$$p_n = -\frac{1}{\tau} + i\omega_{\text{fsr}} n, \quad (33)$$

where  $n$  is integer, and  $\tau$  is the storage time of the cavity,

$$\tau = \frac{2T}{|\ln(r_a r_b)|}. \quad (34)$$

Therefore,  $H_L$  can be written as the infinite product,

$$H_L(s) = e^{sT} \prod_{n=-\infty}^{\infty} \frac{p_n}{p_n - s}, \quad (35)$$

which can be truncated to a finite number of terms for use in control system design.

The response of a Fabry–Perot cavity to laser frequency variations is very different from its response to length variations. Eq. (30) shows that the normalized

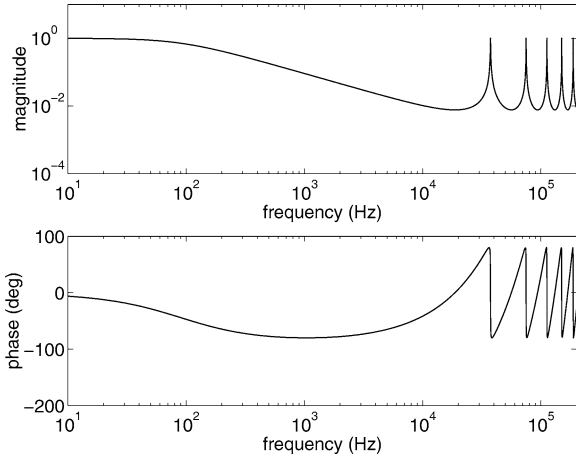


Fig. 3. Bode plot of  $H_L(i\Omega)$  for the LIGO 4-km Fabry-Perot cavities. The peaks occur at multiples of the FSR (37.5 kHz) and their half-widths (91 Hz) is equal to the inverse of the cavity storage time.

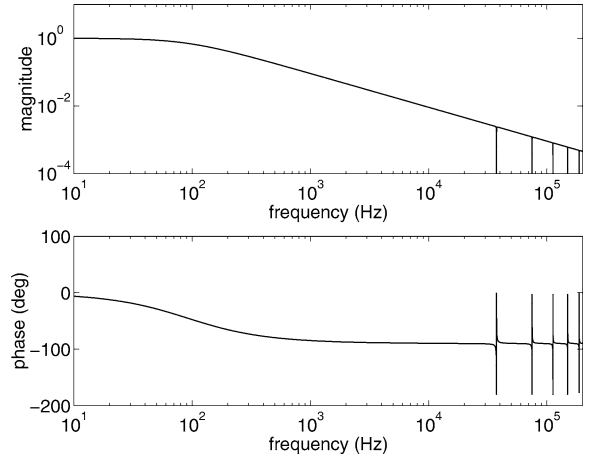


Fig. 4. Bode plot of  $H_\omega(i\Omega)$  for the LIGO 4-km Fabry-Perot cavities. The sharp features are due to the zero-pole pairs at multiples of the FSR.

frequency-to-signal transfer function is given by

$$H_\omega(s) = C(s)H_L(s), \quad (36)$$

or, more explicitly as

$$H_\omega(s) = \left( \frac{1 - e^{-2sT}}{2sT} \right) \left( \frac{1 - r_a r_b}{1 - r_a r_b e^{-2sT}} \right). \quad (37)$$

A Bode plot of  $H_\omega$ , calculated for the same parameters as for  $H_L$ , is shown in Fig. 4. The transfer function  $H_\omega$  has zeros given by Eq. (23) with  $n \neq 0$ , and poles given by Eq. (33). The poles and zeros come in pairs except for the lowest order pole,  $p_0$ , which does not have a matching zero. Therefore,  $H_\omega$  can be written as the infinite product,

$$H_\omega(s) = \frac{p_0}{p_0 - s} \prod'_{n=-\infty}^{\infty} \left( \frac{1 - s/z_n}{1 - s/p_n} \right), \quad (38)$$

where the prime indicates that  $n = 0$  term is omitted from the product.

The zeros in the transfer function indicate that the cavity does not respond ( $\delta E = 0$ ) to laser frequency deviations if these deviations occur at multiples of the cavity FSR. In this case, the amplitude of the circulating field is constant while the phase of the circulating field is changing with the phase of the input laser field.

The cusps in the magnitude of  $H_\omega$  at frequencies equal to multiples of the FSR, such as the one shown

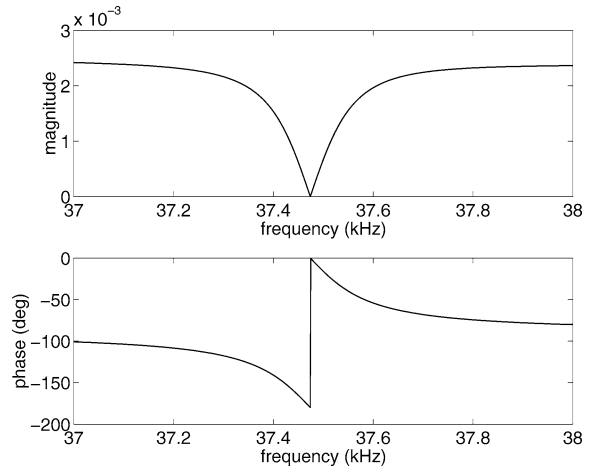


Fig. 5. Bode plot of  $H_\omega(i\Omega)$  in the vicinity of the first FSR for the LIGO 4-km Fabry-Perot cavities.

in Fig. 5, can be utilized for accurate measurements of the cavity length. This technique is being used to measure the length of the 4-km LIGO Fabry-Perot arm cavities. The preliminary results confirm the functional form and sharpness of the cusp predicted by our calculations [18]. Measuring the length in this way can be performed while the cavity is in lock. Alternative methods utilizing linear ramps of the laser frequency across several FSR inevitably disrupt the lock and therefore cannot be used for in-situ measurements.

## 5. Summary

We have derived the exact condition for resonance in a Fabry–Perot cavity when the laser frequency and the cavity length are changing. In contrast to the quasi-static resonance approximation where they appear equally (Eq. (26)), in dynamic resonance changes in the laser frequency and changes in the cavity length play very different roles (Eq. (21)). Maintenance of dynamic resonance requires that the frequency-to-length transfer function,  $C(s)$ , be taken into account when compensating for length variations by frequency changes and vice versa. Compensation for length variations by frequency changes becomes increasingly more difficult at frequencies above the FSR, and impossible at multiples of the FSR where the cavity field does not respond to laser frequency changes.

Cusps in the response of the cavity locking signal to laser frequency variations at these discrete frequencies can be utilized to characterize long resonators. For example, they can be utilized for making measurements of the length of km-scale Fabry–Perot resonators with high precision. Such measurements are presently underway using the 4-km-long arms of the interferometer at the LIGO Hanford Observatory.

As can be seen in Fig. 4, the response of the PDH error signal to laser frequency variations decreases as  $1/\Omega$  for  $\Omega \gg \tau^{-1}$  and becomes zero at frequencies equal to multiples of the cavity FSR. In contrast, the response to length variations is a periodic function of frequency as shown in Fig. 3. For  $\Omega \gg \tau^{-1}$ , it also decreases as  $1/\Omega$  but only to the level of  $(1 + F)^{-1/2}$  returning to its maximum value at multiples of the cavity FSR. Thus, at these selective frequencies the sensitivity to length variations is maximum whereas the sensitivity to frequency variations is minimum.

These characteristics suggest searches for gravitational waves at frequencies near multiples of the FSR. However, because gravitational waves interact with the light as well as the mirrors, the response of an optimally-oriented interferometer is equivalent to  $H_\omega(s)$  and not to  $H_L(s)$  [5]. Thus, an optimally-oriented interferometer does not respond to gravitational wave at multiples of the FSR. However, for other orientations gravitational waves can be detected with enhanced sensitivity at multiples of the cavity FSR [19].

## Acknowledgements

We thank B. Barish, G. Cagnoli, R. Coldwell, and G. Mueller for valuable discussions, and D. Shoemaker and other members of LIGO for editorial comments. This research was supported by the US National Science Foundation under grants PHY-9210038 and PHY-0070854.

## References

- [1] J.M. Vaughan, *The Fabry–Perot Interferometer: History, Theory, Practice, and Applications*, Adam Hilger, Bristol, England, 1989.
- [2] A. Abramovici, et al., *Science* 256 (1992) 325.
- [3] C. Bradaschia, et al., *Nucl. Instrum. Methods Phys. Res. A* 289 (1990) 518.
- [4] J. Camp, L. Sievers, R. Bork, J. Heefner, *Opt. Lett.* 20 (1995) 2463.
- [5] J. Mizuno, A. Rüdiger, R. Schilling, W. Winkler, K. Danzmann, *Opt. Commun.* 138 (1997) 383.
- [6] V. Chikarmane, S.V. Dhurandhar, R. Barillet, P. Hello, J.-Y. Vinet, *Appl. Opt.* 37 (1998) 3236.
- [7] A. Pai, S.V. Dhurandhar, P. Hello, J.-Y. Vinet, *Eur. Phys. J. D* 8 (2000) 333.
- [8] D. Redding, M. Regehr, L. Sievers, *Dynamic models of Fabry–Perot interferometers*. LIGO Tech. Rep. T970227, California Institute of Technology, 1997.
- [9] D. Sigg, et al., *Frequency response of the LIGO interferometer*. LIGO Tech. Rep. T970084, Massachusetts Institute of Technology, 1997.
- [10] B. Bhawal, *J. Opt. Soc. Am. A* 15 (1998) 120.
- [11] R.G. Beausoleil, D. Sigg, *J. Opt. Soc. Am. A* 16 (1999) 2990.
- [12] H. Yamamoto, in: S. Kawamura, N. Mio (Eds.), *Gravitational Wave Detection II*, Proceedings of the 2nd TAMA International Workshop, Universal Academy Press, Tokyo, 2000.
- [13] M.J. Lawrence, B. Willke, M.E. Husman, E.K. Gustafson, R.L. Byer, *J. Opt. Soc. Am. B* 16 (1999) 523.
- [14] M. Rakhmanov, *Appl. Opt.* 40 (2001) 1942.
- [15] M. Rakhmanov, Ph.D. Dissertation, California Institute of Technology, Pasadena, CA, 2000.
- [16] R.W.P. Drever, J.L. Hall, F.V. Kowalski, J. Hough, G.M. Ford, A.J. Munley, H. Ward, *Appl. Phys. B* 31 (1983) 97.
- [17] M. Born, E. Wolf, *Principles of Optics*, Pergamon Press, Oxford, 1980.
- [18] R.L. Savage Jr., *LIGO Hanford Observatory Electronic Log Book*, October 4, 2002.
- [19] R. Schilling, *Class. Quantum Grav.* 14 (1997) 1513.